Available online at www.sciencedirect.com
ScienceDirect
Journal of Solid State Chemistry 180 (2007) 1180–1187
JOURNAL OF SOLID STATE CHEMISTRY
www.elsevier.com/locate/jssc

Porous properties of silylated mesoporous silica and its hydrogen adsorption

Takahiro Takei*, Ohki Houshito, Yoshinori Yonesaki, Nobuhiro Kumada, Nobukazu Kinomura

Center for Crystal Science and Technology, Faculty of Engineering, University of Yamanashi, 7 Miyamae, Kofu, Yamanashi 400-8511, Japan

Received 10 August 2006; received in revised form 8 January 2007; accepted 8 January 2007
Available online 24 January 2007

Abstract

Porous properties of mesoporous silica silylated with various organic silanes were examined and their hydrogen adsorption properties were measured at 77 K. By silylation of the mesoporous silica, the specific surface area, pore radius and pore volume steeply decreased depending on both the size of the silane and the amount actually incorporated into the mesoporous framework. The pores reduced in size depending on the amount of modifying silane and vanished completely in the samples silylated with 3-aminopropyltriethoxysilane and phenyltrichlorosilane. Hydrogen adsorption isotherms of the silylated samples were measured at 77 K. With the exception of the sample with phenyltrichlorosilane, hydrogen adsorption volumes were proportional to the surface area with a slope of around 1.1 molecules/nm^2. On the other hand, for the sample treated with phenyltrichlorosilane, a large hydrogen adsorption volume of around 38.1 molecules/nm^2 was obtained. On heating the silylated compounds at 500 °C, micropores formed and the hydrogen adsorption volume increased by 1.5 times or more due to the development of micropores.

Keywords: Mesoporous silica; Hydrogen adsorption; Silylation; Porous material; Inorganic–organic hybrid

1. Introduction

Mesoporous materials are excellent candidates as an adsorbent for removal of unwanted substances or collection of useful substances. For control of the shape, size and periodic arrangement of the pores, preparations of mesoporous materials by self-assembly of templates have been examined using various organic templates. In the case of mesoporous silica, typical pore structures prepared by self-assembly are hexagonal, cubic and grid arrangements [1–6]. Applications have been investigated for use as molecular sieves, sensing materials, gas separators, ultracapacitor electrodes, catalysts, filters, storage materials and so on [7–11]. For these applications, hybridization with activators is sometimes required to enhance the desired properties. Thus, hybridization of mesoporous silica with metals and organic materials has been examined extensively by many researchers.

Generally, adsorption mechanisms can be classified into two types; physisorption and chemisorption. For physisorption, adsorbate molecules are held on the surface of the adsorbent by only the adsorption potential. In that case, adsorption is reversible. For chemisorption, chemical bonds are formed between the adsorbent and adsorbate molecules, and adsorption may be irreversible. In terms of hydrogen storage, the adsorption mechanism in hydrogen adsorbing metal alloys can be regarded as chemisorption, while that in carbon is physisorption. As for organic materials, crown ethers and phenyl groups have been examined for their hydrogen adsorption capability by computational simulations. [12,13] They have confirmed that these types of organic molecules and groups are probable candidates for hydrogen storage materials. However, as-prepared solid organic materials have very small surface areas, which make it difficult for fast hydrogen adsorption/desorption in large quantities.

*Corresponding author. Fax: +81 55 254 3035.
E-mail address: takei@yamanashi.ac.jp (T. Takei).

0022-4596/$ - see front matter © 2007 Elsevier Inc. All rights reserved.
doi:10.1016/j.jssc.2007.01.013

Therefore, in this paper, mesoporous silica, a high-surface area inorganic framework, was hybridized with various organosilanes instead. These types of hybrid organic–inorganic silica materials have been studied before [14–22]; here, we also examine the pore size/structure and hydrogen adsorption properties of these materials.

2. Experimental section

2.1. Synthesis of mesoporous silica

Synthesis of mesoporous silica was carried out as follows: 1.09 g of hexadecyltrimethylammonium bromide was used as a cationic surfactant for formation of the hexagonal structure. The surfactant was dissolved in distilled water with stirring and 3.1 mL of ethylamine was added to this solution. Then, 5.0 mL of tetraethoxysilane was blended with the mixed solution and was stirred for 10 min. The resultant solution was poured into a Teflon-lined vessel and hydrothermally treated at 110 °C for 48 h. After the hydrothermal reaction, the aggregate were separated and washed by water via suction filtration using an aspirator, and then dried at 50 °C for 24 h. The obtained powder at this point is referred to as meso-structured silica (instead of mesoporous silica), since the pores are assumed to be completely filled with surfactant.

To remove the surfactant, the synthesized meso-structured silica was put into a solution of 80 vol% ethanol and 20 vol% HCl with concentration of 5 mol/L, and was shaken at 40 °C for 12 h. Then, it was separated and washed by ethanol via suction filtration, and dried at 50 °C. The obtained powder is designated as MPS hereafter.

2.2. Silylation

The MPS pore surface were silylated by two different methods: refluxing with organochlorosilane in the absence of water, or shaking in an ethanol solution of organotriethoxysilane. In the former process, the coupling reagents used were vinyl-, (3-chloropropyl)- and phenyltrichlorosilane. Functional groups are abbreviated as Vi-, CP- and Ph-, respectively. For the anhydrous former reaction, the MPS and organochlorosilane (molar ratio 1 to 3) were dissolved in dehydrated toluene under nitrogen atmosphere. The mixed solution was refluxed while bubbling with dry nitrogen gas at 50 °C for 48 h. Then, it was separated and washed by toluene to remove excess silane, and dried at 50 °C. Thus, silylated compounds are designated as ViTC, CPTC and PhTC hereafter. The latter process was performed using vinyl- and (3-aminopropyl)-triethoxysilane. Respective functional groups are abbreviated as Vi- and AP-. Aqueous ammonia solution for catalyzing hydrolysis was added to ethanol. Then, MPS and silane (ratio 1 to 3) were added to the solution. The solution was shaken at 40 °C for 24 h. Then, it was separated and washed by ethanol to remove excess silane and dried at 50 °C. Hereafter, silylated samples are designated as ViTE or APTE, respectively.

In terms of grafting mechanisms, silanol groups presumably on the pore surface of MPS were the modification sites in both processes. For the organotrichlorosilane, the silane can bind to the silanol group directly. For the organotriethoxysilane, the silane tends to bind via a free organosilanol species formed after reaction with water. Reaction equations were shown as follows:

$$\text{Organotrichlorosilane}: \quad \mathrm{Si{-}OH + Cl{-}Si{-}R} \rightarrow \mathrm{Si{-}O{-}Si{-}R + HCl} \quad (\mathrm{R}: \ \mathrm{Vi-},\ \mathrm{CP-}\ \text{or}\ \mathrm{Ph-}),$$

$$\text{Organotriethoxysilane}: \quad \mathrm{Si{-}OH + C_2H_5O{-}Si{-}R + H_2O} \rightarrow \mathrm{Si{-}OH + HO{-}Si{-}R + C_2H_5OH} \rightarrow \mathrm{Si{-}O{-}Si{-}R + C_2H_5OH + H_2O} \quad (\mathrm{R}: \ \mathrm{Vi-}\ \text{or}\ \mathrm{AP-}).$$

These methods possibly pose different pore structures because of the difference of chemical bonding process. That is, the chlorosilane can bind with a silanol group only on MPS, whereas the ethoxysilane can bind not only with MPS but also with each other because of condensation polymerization via hydrolysis of the ethoxysilane. The samples and their synthesis conditions are summarized in Table 1.

From the Van der Waals and covalent radii of H, C, N, Si and Cl atoms, lengths and volumes of the functional group including the Si atom in each silane molecule were estimated and are shown in Table 1. The length and volume are designated as $l_{\mathrm{R-Si}}$ and $v_{\mathrm{R-Si}}$, hereafter.

2.3. Characterization

The degree of the surfactant removal was evaluated by CHN elementary analysis (MT-5, Yanaco). The porous structure of the silylated samples was estimated by powder XRD (RINT2000 V, Rigaku) using graphite monochromated Cu$K\alpha$ radiation. Amounts of organic component were evaluated by differential thermal analysis in the range

Table 1
Synthesis conditions of the hybrids, and lengths and volumes of each functional group including the silicon atom within a silane molecule

Sample	Solvent	Temperature (°C)	Time (h)	Atmosphere	Process	$l_{\mathrm{R-Si}}$ (nm)	$v_{\mathrm{R-Si}}$ (nm^3)
ViTC	Toluene	50	48	N_2	Reflux + stir	0.717	0.068
CPTC	Toluene	50	48	N_2	Reflux + stir	0.934	0.106
PhTC	Toluene	50	48	N_2	Reflux + stir	0.912	0.113
ViTE	Ethanol	40	24	Air	Stir	0.717	0.068
APTE	Ethanol	40	24	Air	Stir	0.956	0.108

from 200 to 700 °C in air atmosphere (TG-DTA, TAS200, Rigaku). Organic and hydroxyl groups in the samples were examined via infrared spectroscopy (FT-IR, FT/IR-410, Jasco). Adsorption isotherms of the silylated samples were obtained using a N_2 gas microporosimeter (BELSORP-mini, Nippon BEL) at 77 K. Pore size distribution and specific surface area were calculated by Dollimore–Heal [23] and BET [24] methods. Pore volume was estimated from the amount of adsorbed N_2 gas at 0.963 in relative pressure, which derives from 25 nm radii pores. Micropore volume was calculated by *t*-plot. H_2 adsorption isotherms were also obtained by a microporosimeter (BELSORP-28, Nippon BEL) at 77 K.

3. Results and discussion

3.1. Porous structures

Before the surfactant extraction, the amount of carbon in the meso-structured silica was around 29.8 mass%. This result implies that the molar ratio of incorporated hexadecyltrimethylammonium cations to SiO_2 was 0.127. After surfactant removal, the amount of carbon decreased to around 1.7 mass% and the molar ratio was 0.004. These results confirm that the treatment succeeded in removing 96% of the surfactant. Since the pores are now hollow, the obtained MPS can be regarded as mesoporous silica. Fig. 1 shows the XRD patterns of silylated samples. Peaks at around 2.1°, 3.6° and 4.2° in 2θ in these patterns are attributed to 100, 110 and 200 diffractions and these samples have a hexagonal structure. The hexagonal type structure was found to have a lattice constant of $a = 4.9$ nm, estimated from these peaks positions. For PhTC and APTE, the peak intensity of the 100 diffraction line decreased upon silylation. Fig. 2 shows the TG curves of the silylated samples. Weight losses in the temperature range at around 100 °C correspond to adsorbed water. MPS had a large loss within the range because of the many silanol groups on the pore walls, whereas the hybrids had smaller losses due to grafted organic groups. The losses in the range from around 200–300 °C correspond to physically adsorbed silane molecules. From these curves, we assume that the hybrids had a small amount of adsorbed silane of around several percent. To estimate the amount of the organic component, weight losses in the temperature range from 200 to 700 °C were used in this paper. In this temperature range, PhTC exhibited the largest weight loss (28 mass%), while ViTC lost the least mass (11 mass%). The weight loss of around 5 mass% between 200 and 700 °C for MPS is attributed to confined H_2O in the SiO_4 network and residual surfactant. Therefore, when finding the true amount of organics from only the grafted organosilane, the weight loss from confined H_2O and residual surfactant must be subtracted from the total weight loss observed between 200 and 700 °C. Table 2

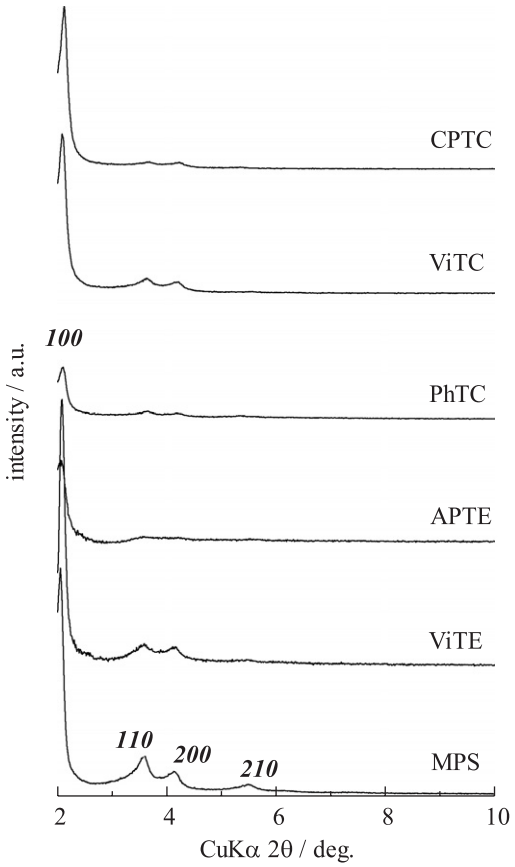

Fig. 1. XRD patterns of mesoporous silica and silylated compounds.

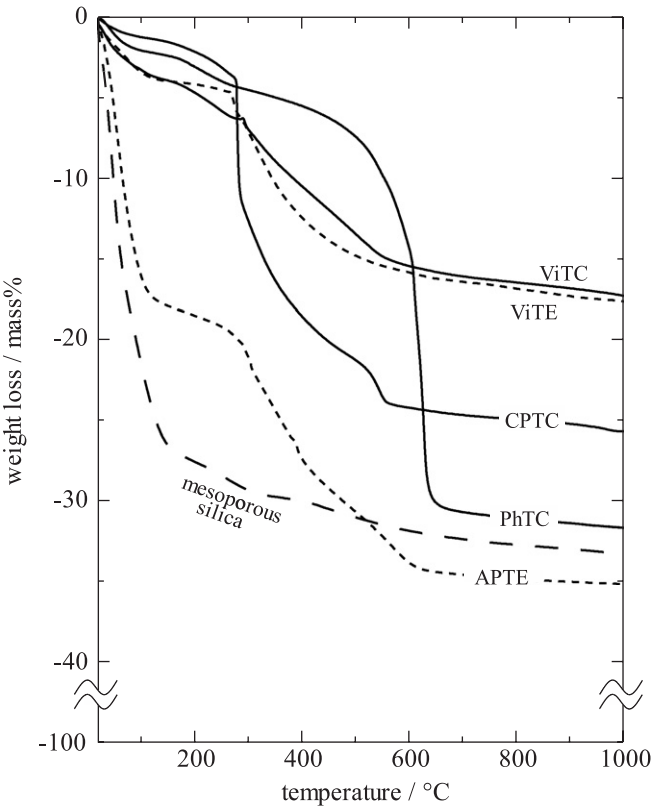

Fig. 2. TG curves of mesoporous silica and silylated compounds.

Table 2
Amount of organic component, mole fraction of organic component, specific surface area and pore volume

Sample	W_{org} (mass%)	R/MPS	S_a ($m^2 g^{-1}$)	V_P ($mL g^{-1}$)
ViTC	3.8	0.143	910	0.49
CPTC	15.7	0.191	730	0.49
PhTC	21.7	0.319	20	0.05
ViTE	4.7	0.183	680	0.39
APTE	13.3	0.227	130	0.10

W_{org}: amount of organic component.

shows the synopsis of amount of organic component, mole fraction of organic component per MPS, specific surface area and pore volume. The term of R/MPS is the molar ratio of deposited silane to MPS. R/MPS of 0.32 for PhTC is larger in particular than those of other samples. No relationship between the molecular size and R/MPS can be confirmed, since the pore size of MPS of around 3 nm in diameter is sufficiently large for induction of any of the silane molecules. It is reasonable that the sample with the largest surface area (ViTC) was grafted with the least amount of silane (smallest R/MPS ratio) while the sample with the smallest surface area (PhTC) has the largest amount of grafted silane.

Fig. 3 shows N_2 isotherms and pore size distributions of silylated samples. MPS had a very sharp distribution at a radius of around 1.51 nm. In the silylated compounds, ViTC, CPTC and ViTE had their maximum distributions at around 1.21, 0.96 and 0.84 nm in radius, respectively. On the other hand, PhTC and APTE showed no noticeable distribution in the mesopore range. Fig. 4 shows the relationships between the product of v_{R-Si} and R/MPS, and their specific surface area, S_a, pore volume, V_P, or pore radius, R_P. The term $v_{R-Si} \cdot R$/MPS is a relative measure of the volume occupied by organosilane for any given amount of grafted MPS. S_a, V_P and R_P of silylated compounds decreased with increasing $v_{R-Si} \cdot R$/MPS, except for CPTC. This confirms that pores are being filled as the amount of silane increases. When $v_{R-Si} \cdot R$/MPS is below 0.015 nm^3, S_a and R_P decreased with a seemingly square root relationship, though, V_P decreased linearly. The tendencies seem to be consistent considering that MPS has one-dimensional pores, because $v_{R-Si} \cdot R$/MPS and V_P have a same dimension of R_P^2; however, S_a has the same dimension of R_P. S_a, V_P and R_P declined as $v_{R-Si} \cdot R$/MPS increased and V_P vanished when $v_{R-Si} \cdot R$/MPS reached 0.024. In other words, the pores are filled up with silane molecules at around $v_{R-Si} \cdot R$/MPS = 0.024. In terms of silane derivative, the pores were filled up when phenyltrichlorosilane and aminopropyltriethoxysilane were used. For ViTC, the S_a, V_P and R_P were obviously larger than those of ViTE. These results seem to be consistent with the difference of chemical bonding process between two kinds of silane. For CPTC, the S_a, V_P and R_P were extraordinary large, compared with its moderate $v_{R-Si} \cdot R$/MPS. This discrepancy certainly implies that the CP- groups reside not only

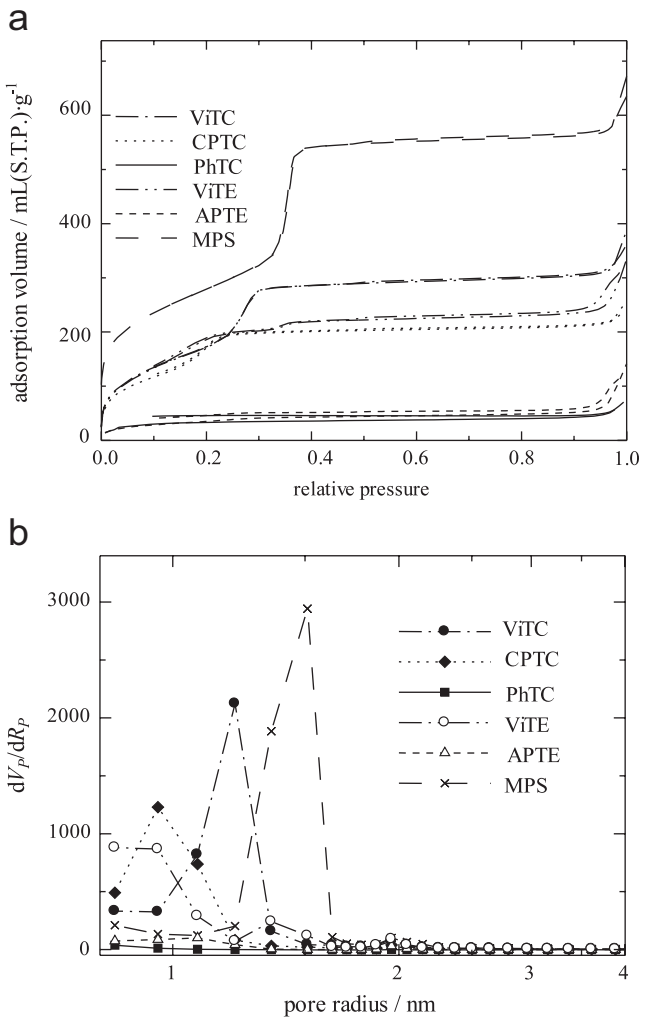

Fig. 3. N_2 isotherms and pore size distributions of silylated mesoporous silica.

in the pore but also on the surface of the MPS grain. V_p is expressed by subtracting the volume of deposited silane within the pores from pore volume of MPS as shown by following formula:

$$V_P = (1 - w - fw)V_{P,MPS} - \left(\frac{fw}{d_{SiO_2}} + \frac{w}{d_R}\right)k,$$

where k is the portion of the organic component which resides in the pores, $V_{P,MPS}$ the pore volume per unit mass of the MPS, w the mass fraction of organic component, f the ratio of molecular weight of SiO_2 to that of the organic component in a deposited silane molecule and d_R and d_{SiO_2} are densities of the organic component in a deposited silane molecule and SiO_2, respectively. In this formula, each term is attributed to the pore volume of MPS and the volume of deposited silane within pores. The d_R and d_{SiO_2} were regarded as 0.89 and 2.2 g/cm^3 from the densities of liquid chloropropane and glassy silica, respectively. Calculation of k for CPTC by the formula implies that 49% of the CP-groups are deposited in the pores of MPS. Fig. 5 shows illustrations of the mesoporous structure of the silylated

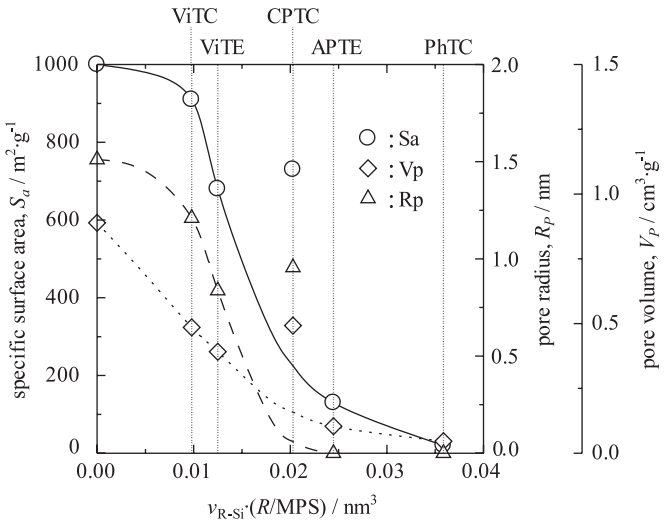

Fig. 4. Dependence of specific surface area, pore volume and pore radius on product of molecular volume (v_{R-Si}) and ratio of organic group to mesoporous silica (R/MPS).

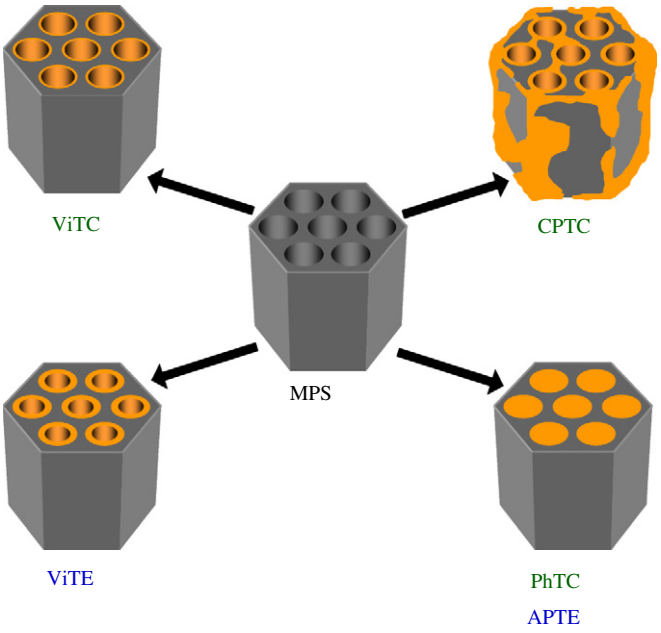

Fig. 5. Scheme of dependence of texture of silylated compounds on different silane molecules.

compounds. Degree of silylation within pores is concluded to be in the order of PhTC > APTE > ViTE ≥ ViTC regardless of the silane molecular size. For CPTC, about half amount of silane deposited on the MPS grain surface outside the pores.

3.2. H_2 adsorption

Fig. 6 shows H_2 isotherms at 77 K below atmospheric pressure. In this figure, they were reversible, indicating physisorption. In the case of MPS, the amount of adsorbed H_2 reached 48 mL (S.T.P)/g, corresponding to 0.4 mass%.

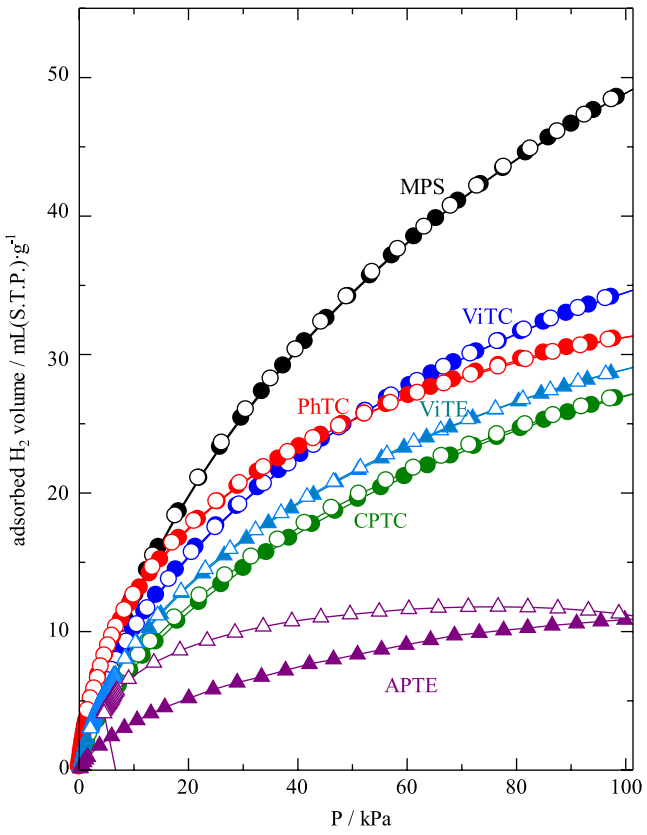

Fig. 6. Hydrogen adsorption isotherms of silylated mesoporous silica.

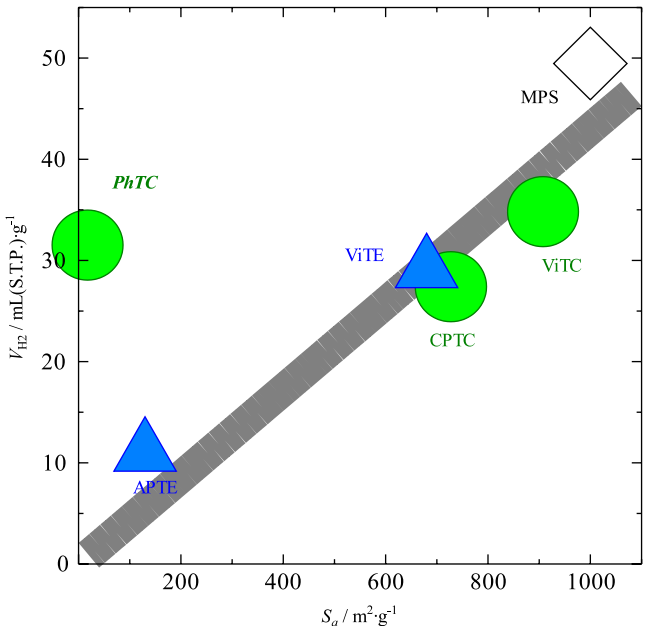

Fig. 7. Relationships between specific surface area and adsorbed H_2 volume at 77 K.

On the other hand, the silylated MPS adsorbed smaller amounts of H_2 than the MPS. Fig. 7 shows relationship between specific surface area measured by N_2 and adsorbed volume of H_2. Other than for PhTC, hydrogen adsorption

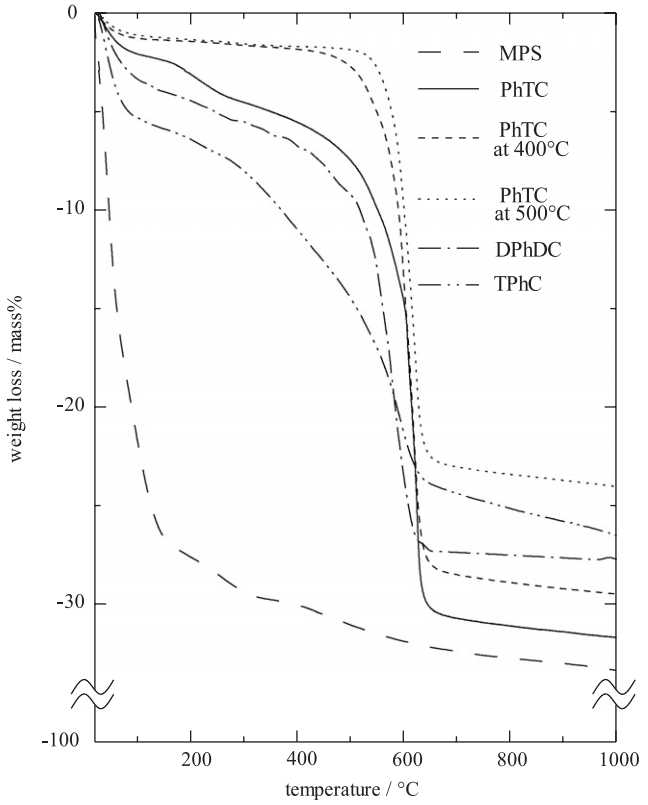

Fig. 8. TG curves of compounds silylated by phenyltrichlorosilane fired at 400 or 500 °C, and silylated by diphenyldichlorosilane and triphenylchlorosilane.

increased proportionally with specific surface areas, independent of the chemical species in the pore. Since the constant of proportion is around 0.0043 mL/m^2, the number of adsorbed H_2 molecules per surface area (the latter measured by N_2) can be calculated to be around 1.1 molecules/nm^2. This calculated number implies conventional physisorption of H_2 molecules on an ordinary solid surface. In the case of PhTC, the adsorbed volume was exceptionally large in spite of its small surface area (measured by N_2 to be around 20 m^2/g). Here, the number of adsorbed H_2 is around 38.1 molecules/nm^2 and is much larger than others. Based on its reversible isotherm, the H_2 molecules in PhTC are adsorbed physically. The large adsorption volume might result from an alternative strong physicochemical interaction between Ph- and H_2, or the existence of ultramicropores which are not accessible by N_2.

PhTC has an aptitude for the H_2 adsorption; however, only small number of adsorbable sites are conceived to be available for H_2 molecules owing to its low specific surface area. In order to investigate the effect of the Ph- group for H_2 adsorption, the amount of the Ph- group in the hybrids were controlled by the firing of PhTC at 400 and 500 °C in air for 2 h, or by silylation of MPS by using diphenyldichlorosilane or triphenylchlorosilane, which are abbreviated as DPhDC or TPhC in this paper. Fig. 8 shows the TG curves of these materials. Amounts of organic component in these materials were estimated by the weight losses between 200 to 700 °C. PhTC pretreated at 400 °C exhibited a weight loss of 20.5 mass% between 200 and 700 °C, while when pretreated at 500 °C the weight loss between 200 and 700 °C decreased to 14.5 mass%. DPhDC samples without pretreatment heated from 200 to 700 °C lost 16.9 mass% of weight, while similar TPhC samples exhibited a 11.8 mass% weight loss.

Fig. 9 shows FT-IR spectra of MPS, PhTC, PhTC fired at 400 and 500 °C, DPhDC and TPhC. In this figure, we can see the vibrations from H_2O, the silanol group and organic moieties; these are the stretching vibration of vicinal silanol groups which hydrogen bonds weakly with each other, $\nu(O–H_{vic})$, at 3700–3100 cm^{-1}; the stretching vibration of the isolated silanol group, $\nu(O–H_{iso})$, at around 3660 cm^{-1}; the bending vibration of water, $\delta(H_2O)$, at 1640 cm^{-1}; the stretching vibration of the C = C bond in an aromatic ring, $\nu(C = C_{aro})$, at 1596 and 1432 cm^{-1}; the out-of-plane bending vibration of the C_6H_5, $\gamma(C_6H_5)$, at 737 and 697 cm^{-1}; and the stretching vibration of the C–H bond ν(C–H), at 3057 and 3010 cm^{-1}, respectively. In the spectrum of MPS, $\nu(O–H_{vic})$ and $\delta(H_2O)$ were observed. In the as-silylated sample, these vibrations decreased and vibrations from organic moieties

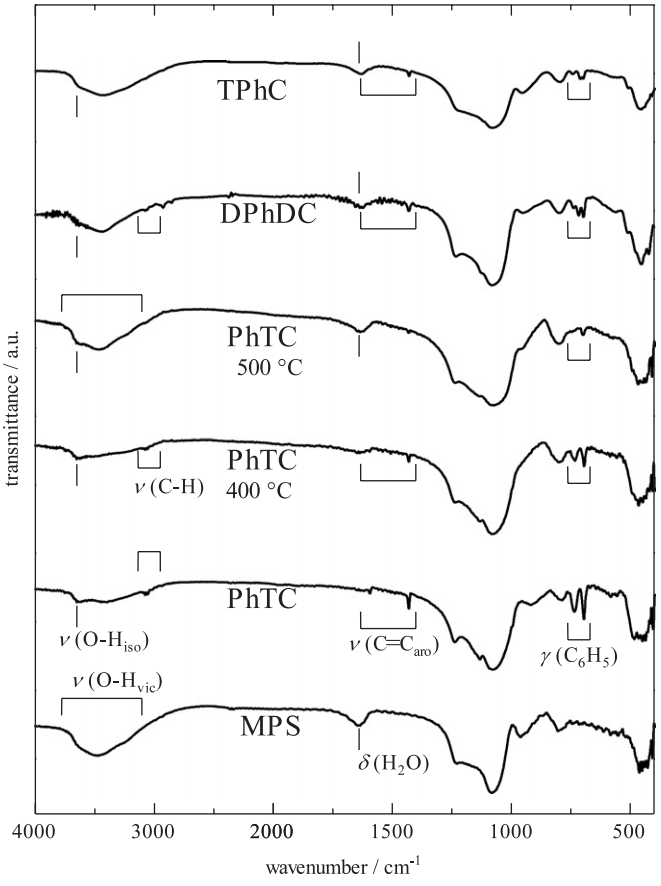

Fig. 9. FT-IR spectra of compounds silylated by phenyltrichlorosilane fired at 400 or 500 °C, and silylated by diphenyldichlorosilane and triphenylchlorosilane.

Table 3
Amount of organic component, pore properties and hydrogen adsorption volumes of as-silylated and fired PhTC samples

	W_{org} (mass%)	S_a ($m^2\,g^{-1}$)	$V_{P,micro}$ ($mL\,g^{-1}$)	$V_{P,meso}$ ($mL\,g^{-1}$)	V_{H_2} ($mL\,g^{-1}$)
PhTC	21.7	20	0.002	0.044	31.4
PhTC at 400 °C	20.5	139	0.052	0.047	33.5
PhTC at 500 °C	14.5	545	0.161	0.043	52.1
DPhDC	16.9	626	—	0.384	35.5
TPhC	11.8	911	—	0.654	45.2

appeared. For DPhDC and TPhC, a small $\gamma(C_6H_5)$ absorption band were observed but $\nu(O–H_{vic})$ and $\delta(H_2O)$ still remained, indicating that a limited number of silanol groups were replaced with diphenyl or triphenyl groups, due to the fairly large surface areas of the supports. The vibrations $\nu(O–H_{vic})$ and $\delta(O–H_{iso})$ decreased for PhTC, and $\nu(O–H_{iso})$ as well as $\nu(C=C_{aro})$ and $\gamma(C_6H_5)$ appeared instead, because some silanol groups were substituted with Ph- groups which weakened hydrogen bonding of surface silanol groups. For PhTC fired at 400 °C, absorption bands of $\nu(O–H_{iso})$, $\nu(C–H)$, $\nu(C=C_{aro})$ and $\gamma(C_6H_5)$ were sustained. However, by firing at 500 °C, absorption bands of bands of $\nu(C–H)$ and $\nu(C=C_{aro})$ disappeared and $\gamma(C_6H_5)$ decreased, whereas $\nu(O–H_{vic})$ and $\delta(H_2O)$ appeared again. Therefore, we concluded that parts of the Ph- moieties are partially decomposed by firing at high temperature and are replaced with silanol groups which hydrogen bond with each other and H_2O molecules.

Next, the pore structure of these hybrids modified with Ph–silane was investigated in detail. Table 3 shows the amount of organic component W_{org}, specific surface area S_a, micropore and mesopore volumes $V_{P,micro}$ and $V_{P,meso}$, and hydrogen adsorption volumes V_{H_2}, of the as-silylated PhTC, fired PhTC, as silylated DPhDC and TPhC samples. In comparison to PhTC, V_{H_2} increased by firing or silylating using diphenyldichlorosilane or triphenylchlorosilane. Therefore, adsorption efficiency should be investigated by using not only adsorption ability of Ph- group but also micropore filling.

In the case of fired PhTC at 400 and 500 °C, a lot of micropores were formed. From Table 3, while $V_{P,meso}$ was unchanged, S_a and $V_{P,micro}$ increased depending on decrease of amount of organic component. These volume changes indicate that Ph- groups occupying mesopores possibly decomposed partially to form micropore-like wormholes due to the decrease of amount of Ph- groups and the increase of the micropores. In the case of DPhDC or TPhC, the mesopores were not occupied completely and the micropores did not form. With the focus on H_2 adsorption, the V_{H_2} increased drastically by firing the PhTC at 500 °C. This acceleration mechanism is allowed to be investigated as follows.

Generally, adsorption is composed of physisorption, micropore filling and physicochemical interaction on surface. Therefore, the H_2 adsorption volume, V_{H_2}, can

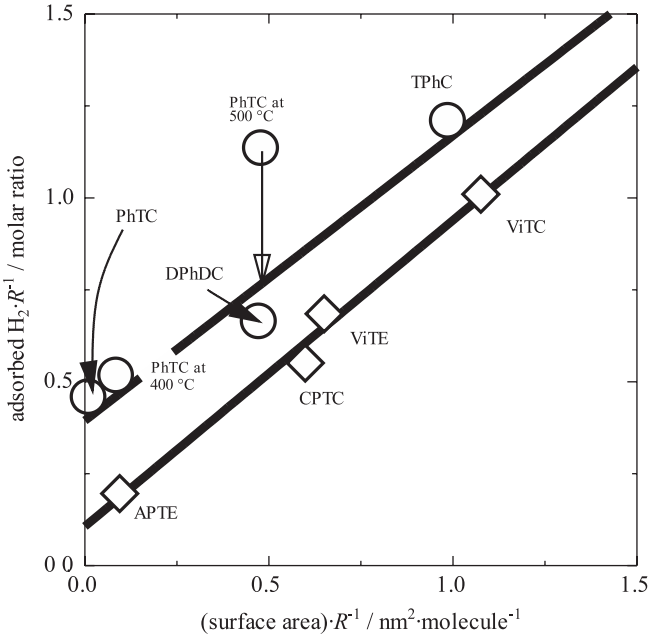

Fig. 10. Dependence of amount of adsorbed H_2 per organic component on surface area per organic component.

be expressed theoretically as $(\alpha S_a + \beta V_{p,micro} + \gamma M_R)$. In this equation, α, β and γ are intensive constants indicating strengths of respective interactions of the physisorption, micropore filling and physicochemical interaction. M_R indicates the molar amount of organic component per sample weight. Here, by dividing both sides of the above equation by M_R, the following relation can be found:

$$\frac{V_{H_2}}{M_R} = \alpha\frac{S_a}{M_R} + \beta\frac{V_{P,micro}}{M_R} + \gamma.$$

If micropore filling can be ignored, dependence of V_{H_2}/MR on S_a/M_R should be linear. Fig. 10 shows relationship between (surface area)/M_R and molar ratio of adsorbed H_2/M_R. In these plots, the samples which have some Ph- groups were plotted on a linear line except for PhTC fired at 500 °C, while others were lumped together. The plots of the sample with Ph- groups confirm that there are no ultramicropores in the PhTC. The constants α and γ of the Ph- related samples were estimated as 0.78 molecule/nm^2 and 0.40, respectively, while those of others were calculated as 0.83 molecule/nm^2 and 0.11, respectively. As

for the constant of physicochemical interaction, γ, H_2 physicochemical interaction on the Ph- group is around 3.7 times as strong as that of others. On the other hand, regarding the constant of physisorption, α, H_2 physisorption occurs on any organic group in comparable level within the range of this paper.

Concerning micropore filling, it came to our attention that the plot of PhTC fired at 500 °C far exceeded above the plots of the other Ph- related samples. This increase probably results from micropore filling. In the case of PhTC fired at 500 °C, around 32% of H_2 adsorption is found to come from micropore filling.

Consequently, Ph- groups have strong capability for physicochemical interaction with H_2, while subsequent physisorption on Ph- groups occurs just like physisorption on the other organic groups. In the case of PhTC fired at 500 °C, many micropores pumped up the H_2 adsorption volume by micropore filling.

4. Conclusions

Silylation of mesoporous silica was carried out by using various silanes having vinyl-, chloropropyl-, phenyl- and aminopropyl- groups, and their porous structures were examined. Organic silane molecules could have been attached chemically on walls of pores to change the porous structure. Hydrogen adsorption of these silylated silicas were also examined at 77 K. The following results were obtained:

(1) The specific surface area, pore volume and pore radius decreased depending as the calculated volume occupied by grafted organosilane ($v_{R-Si} \cdot (R/MPS)$) increased.
(2) The pores became smaller via silane modification and disappeared completely by using APTE or PhTC.
(3) With the exception of PhTC, hydrogen adsorption volume had a proportional correlation on their surface area with slope of around 1.1 molecules/nm^2. Extraordinary large adsorption volumes of around 38.1 molecules/nm^2 were observed in the case of PhTC.
(4) For PhTC, micropores formed during firing at 500 °C and hydrogen adsorption increased from 31 to 52 mL (S.T.P)/g.
(5) The physicochemical interaction on phenyl groups was around 3.7 times stronger than on the other groups.

References

[1] Q. Huo, R. Leon, P.M. Petroff, G.D. Stucky, Science 268 (1995) 1324–1327.
[2] M. Kruk, M. Jaroniec, Chem. Mater. 11 (1999) 2568–2572.
[3] Y. Sakamoto, M. Kaneda, O. Terasaki, D.Y. Zhao, J.M. Kim, G. Stucky, H.J. Shin, R. Ryoo, Nature 408 (2000) 449–453.
[4] M. S. Morey, S. O'Brien, S. Schwarz, G. D. Stucky, 12 (2000) 898–911.
[5] M. Kruk, M. Jaroniec, C.H. Ko, R. Ryoo, Chem. Mater. 12 (2000) 1961–1968.
[6] T. Shigeno, K. Inoue, T. Kimura, N. Katada, M. Niwa, K. Kuroda, J. Mater. Chem. 13 (2003) 883–887.
[7] A. Sayari, Chem. Mater. 8 (1996) 1840–1852.
[8] I. Honma, H.S. Zhou, Adv. Mater. 10/18 (1998) 1532–1536.
[9] M. Vallet-Regi, A. Rámila, R.P. del Real, J. Pérez-Pariente, Chem. Mater. 13 (2001) 308–311.
[10] B. Lindlar, A. Kogelbauer, R. Prins, Microporous Mesoporous Mater. 38 (2000) 167–176.
[11] P.V.D. Voort, E.F. Vansant, Microporous Mesoporous Mater. 38 (2000) 385–390.
[12] S.-H. Jhi, Microporous Mesoporous Mater. 89 (2006) 138–142.
[13] F.M. Mulder, T.J. Dingemans, M. Wagemaker, G.J. Kearley, Chem. Phys. 317 (2005) 113–118.
[14] V. Antochshuk, M. Jaroniec, Chem. Mater. 12 (2000) 2496–2501.
[15] X.S. Zhao, G.Q. Lu, J. Phys. Chem. B 102 (1998) 1556–1561.
[16] V. Goletto, V. Dagry, F. Babonneau, Mater. Res. Soc. Symp. Proc. 576 (1999) 229–234.
[17] T. Takei, R. Kanamori, N. Kumada, N. Kinomura, J. Soc. Inorg. Mater. Japan 8 (2001) 441–446.
[18] M.H. Lim, A. Stein, Chem. Mater. 11 (1999) 3285–3295.
[19] A. Stein, B.J. Melde, R.C. Schroden, Adv. Mater. 12/19 (2000) 1403–1419.
[20] A. Sayari, S. Hamoudi, Chem. Mater. 13 (2001) 3151–3168.
[21] T. Takei, K. Yoshimura, N. Kumada, N. Kinomura, J. Porous Mater. 12 (4) (2005) 337–343.
[22] C.-F. Nie, R. Zhao, J.-S. Suo, J. Porous Mater. 11 (2004) 141–146.
[23] D. Dollimore, G.R. Heal, J. Colloid Interface Sci. 33 (1970) 508–519.
[24] S. Brunauer, P.H. Emmett, E. Teller, J. Am. Chem. Soc. 60 (1938) 309–319.